

図 10: 生理食塩水中での刺激デバイス動作.

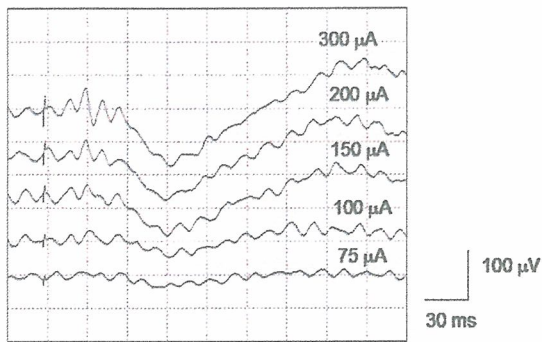


図 11: EEP 実験結果.

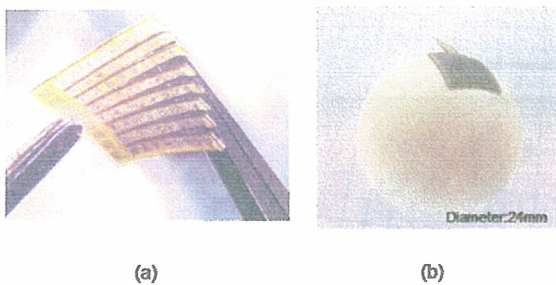


図 12: 576 モックアップ写真. (a) 垂直スリットにより 3 次元のな屈曲性確保. (b) 人眼球に沿う柔軟性.

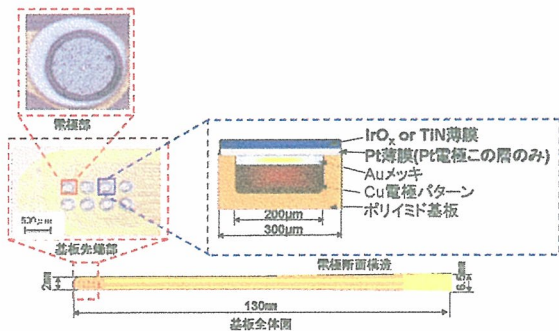


図 13: 電極材料評価用デバイス外観.

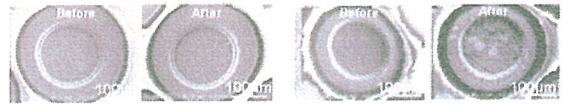


図 14: TiN 薄膜電極と IrOx 薄膜電極の通電前後の表面形態.

厚生労働科学研究費補助金（感覚器障害研究事業）
分担研究報告書

網膜刺激型電極による人工視覚システムの研究開発

分担研究者 小澤素生 株式会社ニデック 副社長

研究要旨

脈絡膜上—経網膜刺激方式(Supra-choroidal transretinal stimulation)の人工視覚システムの開発を目的として、試作機を完成させ評価を行い、実用化に向けての課題抽出と要素技術の開発を行なった。試作機の開発では、基本的な機能を問題なく動作させることができ、仕様上の課題、性能上の課題、製作プロセス上の課題を明確にできた。実用化に向けた要素技術開発では、耐久性の点から刺激電極の構造を抜本的に見直す必要があった。臨床応用が可能なように、安全性に対する性能仕様を向上させるとともに、機能仕様を追加する必要があり、それぞれの要素技術開発を進めている

A. 研究目的

(1) 試作機の開発と評価試験

脈絡膜上—経網膜刺激方式(Supra-choroidal transretinal stimulation: 以降STS方式と記す)に対応した人工視覚システムの実現に向けて要素技術を開発しそれらを組み合わせて、試作機を開発する。この試作機を用いて、評価を行い、実用化に向けての課題を抽出する。

(2) 実用化のための要素技術

実用化のためには、10年以上の長期間にわたって機能と安全性を維持し続ける必要がある。試作機の評価を元にして、刺激電極、ハーメチック・ケース、体内ケーブル、安全性の高い電気回路構成等のさらなる要素技術の開発を行う。

B. 方法と結果

(1) 試作機の開発と評価試験

STS方式に対応した人工視覚システムの実現に向けて要素技術を開発した。それらを用い

てSTS方式の試作機を試作した。図1～3に示すように、体内装置(図1)、体外装置(図2)および制御ソフト(図3)から構成される。体内装置は、本体と電極選択機能(マルチプレクサ: 以下MUX)を含む刺激電極部および硝子体電極がケーブルで接続された構造を有している。一方体外装置は本体、バイザーカメラおよび1次コイルから構成されている。これらを今までに蓄積した要素技術を用いて試作した。

(1)-1. 用いた要素技術

(1)-1-1. RF電力伝送ならびに通信における要素技術

電力伝送系において交番磁界の周波数を高くし、電力伝送と通信を同じ回路系を使用することでユニットの簡略化、軽量化を図った。人体への影響や他の機器への影響を考慮し、高周波の交番磁界の周波数を16.64MHzに決定した。様々な巻き数でコイルを作成した結果、送信コイルは3ターン、受信コイルは6ターンが

体外装置本体とカメラを内蔵したバイザー、1次コイル、動作確認および訓練用PCで構成される。体外装置本体には制御用ボードコンピュータと電力伝送通信用ドライバーボード、電源制御ボード、リチウム電池からなる。体外装置本体のサイズは腰に装着することを考慮して可能な限り小型化した。外出を考慮して電池の持続時間は8時間とし、また、長時間の使用を考慮してACアダプタによる使用と充電も可能なように設計した。(図2)

(2) 実用化のための要素技術

(2)-1. 刺激電極

従来、厚さ $0.2\mu\text{m}$ 程度の白金薄膜を用いた刺激電極が内外で開発されてきた。このような薄膜電極は微細構造が作成しやすいという利点を有するが、その耐久性は必ずしも明らかではなかった。実際に白金薄膜を用いた評価用電極を作成し1週間通電後の電極表面を観察した結果、大半の電極において白金の溶出が生じていた。また電荷注入能力についても、文献値から期待した値の50~80%程度の値しか得られなかった。以上の結果から、薄膜技術で作成した刺激電極の実用化は困難であると結論した。

上記の評価実験で得られた知見をもとに、長期信頼性を実現可能かつ現実的に作製可能な電極構造を考案した。電極は白金のバルク材からなるリベットとワッシャから構成され、リベット先端部を塑性変形させることでリベットとワッシャを固定する。薄膜電極と比較して電極材料となる白金の体積が極めて大きいことから、溶出によって電極が消失するといった致命的な問題は起こりにくいことが期待される。白金のリベットおよびワッシャについて各種形成方法を検討したところ、切削加工を用いて必要な

形状を実現可能であることが明らかになった。この部品を用いてリベット部の塑性変形加工可否を検証したところ、限界はあるものの目指す形状を実現できる見通しが得られた(図12)。続いて、上記電極に接続する配線の形成方法を検討した。配線については、厚さ $10\sim 30\mu\text{m}$ の白金箔を切断して配線パターンを形成する手法を検討した。複数の加工方法を比較検討したところ、フェムト秒レーザーを用いることで必要な配線形状を精度良く加工できる見通しが得られた(図13)。

絶縁層としてはパリレンが第一候補であり、白金箔が2枚のパリレンで挟まれた構造の電極アレイの作成を目指しているが、この2枚のパリレン層間に水分が侵入すると所望の電気刺激ができなくなる。そこでパリレン層間の密着力を評価したところ、適切な熱処理を加えることにより、パリレン層間の密着力を向上させることが可能であることが明らかとなった。これらの技術を集約して評価用1極電極を作成し、生理食塩水中での1週間連続通電評価を実施した。通電前後で電極形状に異常は見られなかった。

(2)-2. ハーメチック・ケース

体内装置の電気回路は、これが生体と接触しないように、十分な気密性能を有するケースに入れる必要がある。STS方式試作機で用いたケースでは、ケース外への配線引き出し部において十分な気密性が確保されないという問題がわかった。そこでケースの基本構造として、ケース本体を生体適合材料として実績のあるSUS316Lで製作し、ケース外との電気接続用に気密端子を溶接により設置し、内部へ電気回路基板を配置・配線後に、ケースを溶接で密封する構造とした。絶縁気密封止材と

して、SUS316L材に熱膨張率が近く有害重金属を含まないRoHS対応低融点ガラスを採用し、どちらもSUS316L材から成るハウジングと貫通電極による単芯気密端子(外径φ1.6mm)(図14)を試作した。性能目標は、以下の気密性と、DC100V 1000MΩ以上の絶縁性能であり、気密端子として達成できた。

さらに、MUXを生体安全な材料から成る微小ケースに収める必要があり、Ni等の有害物質を含まないアルミナ・セラミックをベースとするICパッケージの開発を進めている。白金貫通電極を持つセラミック・ケースにMUX ICをフリップチップ実装し、生体安全な金属リッドを溶接等の方法で接合する事で、ハーメチック・パッケージを構成する。内部にフリップチップ実装が可能な平坦度をもつ薄型セラミック・ケースの開発と、セラミック・ケース上のメタライズと生体安全な金属リッドを接合する方法の検討を進めている。

(2)-3 体内ケーブル

試作機に用いられた体内ケーブルは、十分な伸縮性が確保できなかった。そこでシリコンのコアにパリレンコートされたワイヤーを螺旋状に巻き付けてシリコン・ディッピングする製作工程に変更した。ワイヤー材には白金イリジウム線を用いた。これにより外形φ1.5mmで十分な伸縮性のあるケーブルへ改良することができた(図15)。

(2)-4. 電気回路の安全性向上

生体の安全確保のためには、生体に対して直流電流が流れてはいけない。そこで、体内装置の本体部と刺激電極部を接続するケーブルに対して直流電圧が印加されない回路構成を考案した。試作機ではMUXへ電源を供給

するワイヤーに対し直流を印加していた。また、MUXを制御するための信号も、論理信号のため直流成分を含んでいた。このMUXへの電源供給と制御信号を、まとめて交流信号化するために、制御信号を周波数変調により重畳した交流電源回路を考案した。MUXの動作電圧は、刺激出力回路の電源電圧以上が必要であるため、15Vに設定した。この電圧に対して、ワイヤーの絶縁性能が劣化して生体に接触したとしても半波あたりの電荷注入量が安全な範囲となるよう、搬送周波数は1MHzに設定した。これはMUXを制御するために必要なデータを転送するキャリアとしても十分なものである。

もしもシステム内で配線の断線もしくは絶縁不良が発生した場合、体内装置の配線間インピーダンスが通常動作時とは大きく異なる値を取ることで、それぞれの配線間インピーダンスから故障箇所および故障状態の判別ができる。この原理を応用し、体内装置本体部と刺激電極部間の接続ワイヤーの絶縁不良、もしくはMUXと刺激電極間配線の絶縁不良または断線が発生した場合に、体内装置が動作を停止して安全を確保できるように配線間インピーダンス計測回路を組み入れる検討をおこなった。

C. 考察

(1) 試作機の開発と評価試験

STS方式の試作機として、基本的な機能(RF電力伝送、通信、刺激)は問題なく動作した。一方、実用化していく上での課題も明らかにすることができた。①体内装置本体のサイズが大きい、②MUX部が気密封止されていない、③自己診断機能が十分でない等の人体への埋植に適さない仕様上の課題や、④体内装置

本体の気密性が十分でない、⑤刺激電極の耐久性が不足する等の性能上の課題、また⑥100チャンネル刺激電極の歩留のような製作プロセス上の課題等である。

今後実用化に向けて、抜本的なブレークスルーを必要とする点、改良によって克服する点と、それぞれの課題に対して最適な方向を検討してゆく。

(2) 実用化のための要素技術

STS方式実用化に向けて、各要素技術の検討課題を以下に示す。

(2)-1. 刺激電極

白金は一般的な工業材料ではなく、切削加工や塑性変形加工に関する知見は少ない。しかしながら適切な加工条件のもとでは仕様通りの形状を実現することができた。パリレン層間の密着力評価を通じて、熱処理による密着力向上を比較的容易に評価することができた。しかしこれはあくまで簡易評価であり、最終的には生体内環境下でも密着力が保持され、配線間でのショート等の問題が発生しないことを確認する必要がある。評価用1極電極の通電評価を通じて、少なくとも1週間程度の耐久性を有することが確認できた。今後電極形状の改善を加えるとともに、より長期間にわたる評価を実施することで長期間の耐久性を実証してゆきたい。

(2)-2. ハーメチック・ケース

刺激回路用のケースにおける気密端子の封止材料として低融点硝子を使用しており、ケースに気密端子を溶接する際に熱の影響を受け、性能の劣化が生じないかを気密試験により確認する必要がある。また、絶縁封止材料の生物学的安全性評価として、医療機器GLPにて細胞毒性試験の評価を実施中である。

MUX用の薄型セラミック・ケースの開発はセラミック専業メーカーにて製作を進めている。密封方法について、 $t=10\mu\text{m}$ の白金箔を接合材としてチタン製リッドを溶接することで、十分な気密性が保てるかを試行中である。

(2)-3. 体内ケーブル

試作したケーブルを評価したところ、螺旋状の芯線ピッチの不揃い、シリコーン皮膜の厚さムラ等の問題がわかった。製作工程を改善してこれらのばらつきが生じない対策を施した上で、繰り返し曲げ耐久試験を実施し、耐久性評価を行なう予定である。

(2)-4. 電氣的構成

臨床実験に不可欠な生体の安全性を確保するための要素回路技術が凡そ確立された。さらに実用化のための筐体小型化およびRF送信電力低減の要求を満たすために、専用のICの仕様策定および設計を進めた。今後はICの試作、機能評価および基板実装を行い、体内装置の機能検証を行なう。

D. 健康危惧情報

特になし。

E. 研究発表

1. 論文

Yasuo Terasawa, Hiroyuki Tashiro, Akihiro Uehara, Tohru Saitoh, Motoki Ozawa, Takashi Tokuda and Jun Ohta, "The development of a multichannel electrode array for retinal prostheses" J. of Art. Org., vol.9, No.4, pp.263-266, 2006.

2. 総説

鐘堂健三「人工視覚(4)脈絡膜上 - 経網膜刺激方式人工視覚システム」臨床眼科 2005

3. 学会発表

①齊藤徹、寺澤靖雄、小澤素生「人工視覚システムにおけるイオンマイグレーションの防止」第44回日本生体医工学会、2005年4月27日、ポスター、つくば市

②寺澤靖雄、田代洋行、小澤素生「人工視覚システムにおける白金薄膜電極の電荷注入能力評価」第44回日本生体医工学会、2005年4月27日、ポスター、つくば市

③田代洋行、寺澤靖雄、中谷正義、小澤素生「人工視覚システムの生体内電極インピーダンス計測系の確立」第44回日本生体医工学会、2005年4月27日、ポスター、つくば市

④田代洋行、寺澤靖雄、中谷正義、長原美樹、小澤素生、中内一揚、不二門尚、田野保雄「人工視覚システムの安全性評価のための中期的慢性通電下における電極インピーダンス計測」第43回日本人工臓器学会、2005年12月1日、ポスター、東京都

④寺澤靖雄、田代洋行、上原昭宏、斎藤徹、小澤素生、徳田崇、太田淳「人工視覚システムにおける多極電極の開発」第43回日本人工臓器学会、2005年12月1日、ポスター、東京都

寺澤 靖雄, 田代 洋行, 小澤 素生, 「人工視覚システムにおける白金バンプ電極の電荷注入能力評価」 Tran. of Jpn. Soc. for Med. and Bio. Eng., vol.44, Suppl.1, pp.496, 2006.

F. 知的財産権の出願・登録状況

- ① 特願2004-227491 整流回路及びこれを備えた視覚再生補助装置

- ② 特願2004-348154 視覚再生補助装置
③ 特開2004-298298 視覚再生補助装置
④ 特開2004-298299 視覚再生補助装置
⑤ 特願2005-232878 視覚再生補助装置
⑥ 特願2005-287948 視覚再生補助装置
⑦ 特願2006-3090 視覚再生補助装置
⑧ 特願2006-28963 負荷変調通信回路およびこれを備えた視覚再生補助装置
⑨ 特願2006-58561 視覚再生補助装置
⑩ 特願2006-237007 視覚再生補助装置
⑪ 特願2006-268675 視覚再生補助装置

【図表】

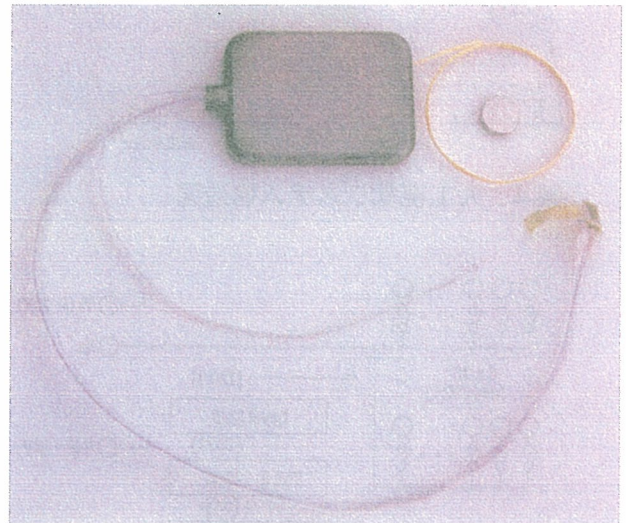


図 1. 体内装置



図 2. 体外装置

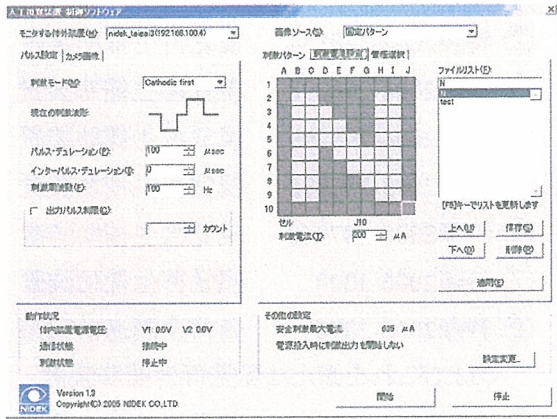


図 3. 制御ソフト

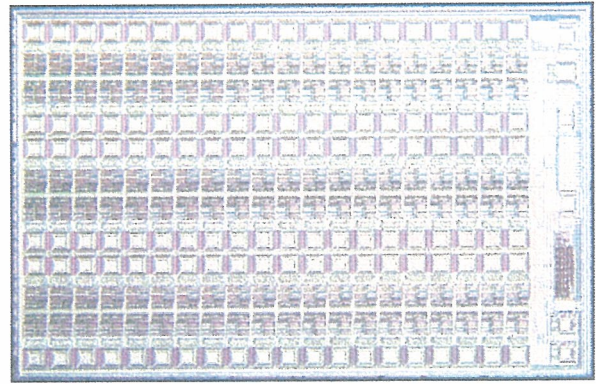


図 6. チップ写真

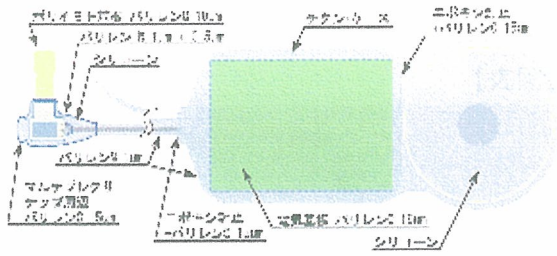


図 4. 人工視覚システム構造図

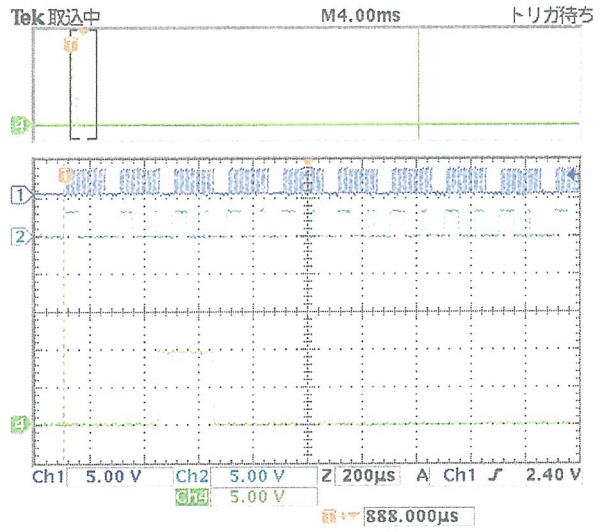


図 7. Iout1 端子の動作波形

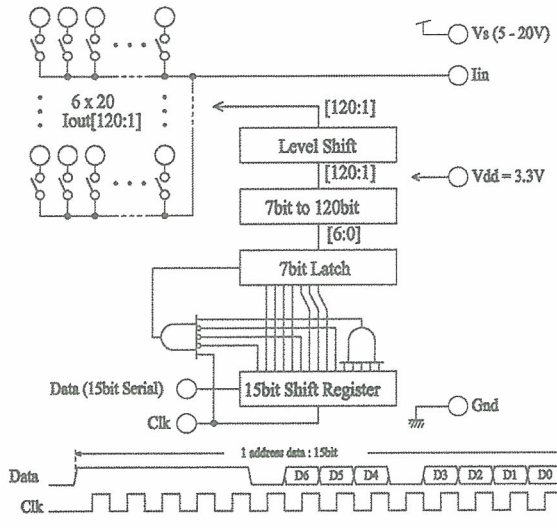


図 5. ブロック図

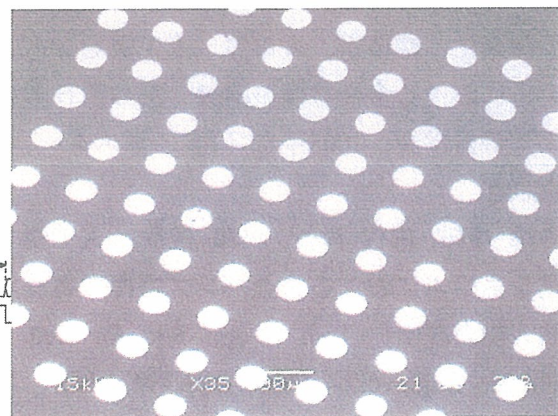


図 8. 刺激電極の SEM 像

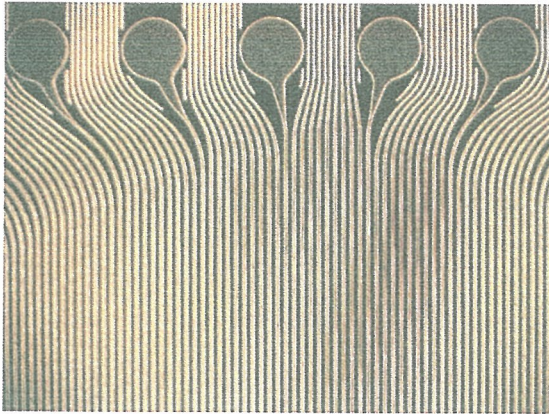


図 9. 金の微細配線パターン

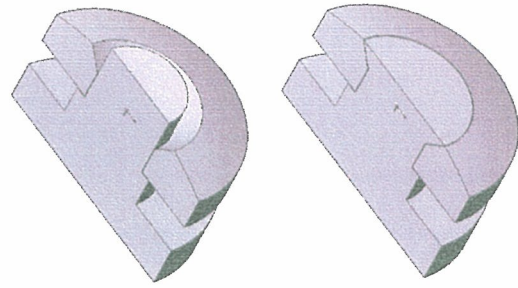


図 12 バルク電極の構造

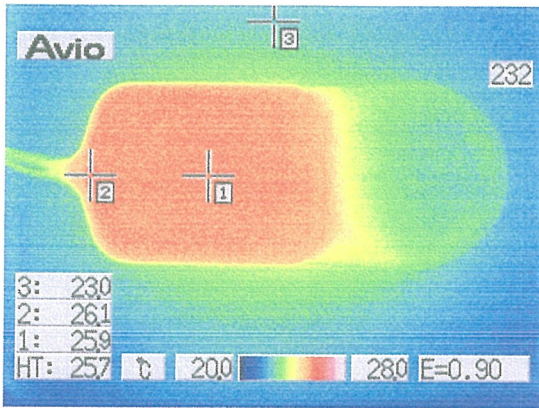


図 10 体内装置の温度上昇分布

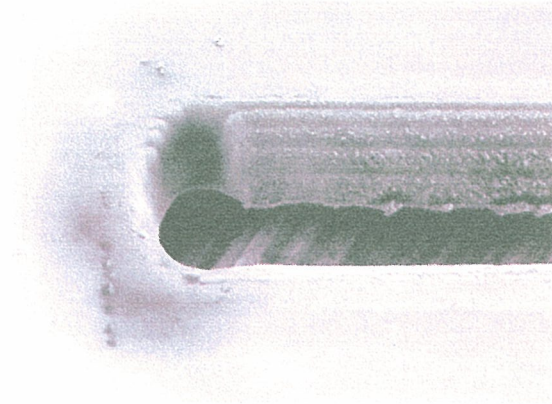


図 13 フェムト秒レーザーによる白金箔切断加工

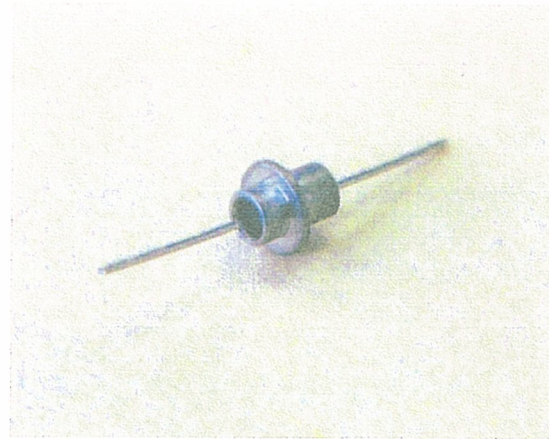


図 14 単芯気密端子

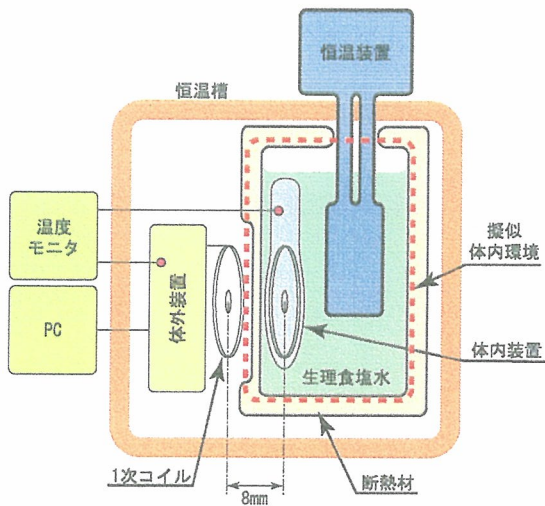


図 11 温度変化におけるシステムの動作状況評価系

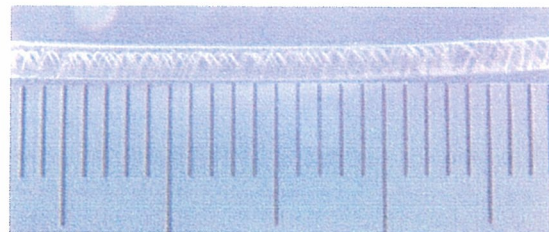


図 15 外形φ1.5mm伸縮性ケーブル

1. Kanda H, Morimoto T, Fujikado T, Tano Y, Fukuda Y, Sawai H.
Electrophysiological studies of the feasibility of suprachoroidal-transretinal stimulation for artificial vision in normal and RCS rats. Invest Ophthalmol Vis Sci. 2004;45:560-6.
2. Sakaguchi H, Fujikado T, Fang X, Kanda H, Osanai M, Nakauchi K, Ikuno Y, Kamei M, Yagi T, Nishimura S, Ohji M, Yagi T, Tano Y. Transretinal electrical stimulation with a suprachoroidal multichannel electrode in rabbit eyes. Jpn J Ophthalmol. 2004;48:256-261.
3. Nakauchi K, Fujikado T, Kanda H, Morimoto T, Choi JS, Ikuno Y, Sakaguchi H, Kamei M, Ohji M, Yagi T, Nishimura S, Sawai H, Fukuda Y, Tano Y..: Transretinal electrical stimulation by an intrascleral multichannel electrode array in rabbit eyes. Graefes Arch Clin Exp Ophthalmol. 2005;243:169-174
4. Morimoto T, Miyoshi T, Matsuda S, Tano Y, Fujikado T, Fukuda Y..: Transcorneal electrical stimulation rescues axotomized retinal ganglion cells by activating endogenous retinal IGF-1 system. Invest. Ophthalmol. Vis Sci.2005;46:2147-2155.
5. Fujikado T, Kanda H, Kusaka S, Nakauchi K, Ozawa M, Matsushita K, Matsushita K, Sakaguchi H, Ikuno Y, Kamei M, Tano Y. Evaluation of phosphene by extraocular stimulation in normals and by suprachoroidal-transretinal stimulation in patients with retinitis pigmentosa. Graefes Arch Clin Exp Ophthalmol, E-Pub, 2007
6. Nakauchi K, Fujikado T, Kanda H, Kusaka S, Ozawa M, T, Sakaguchi H, Ikuno Y, Kamei M. Tano Y. Threshold suprachoroidal-transretinal stimulation current resulting in retinal damage in rabbit. J Neural Eng. 2007;4:S50-S57
7. Morimoto T, Fukui T, Matsushita K, Okawa Y, Shimojyo H, Kusaka S, Tano Y, Fujikado T. Evaluation of residual retinal function by pupillary constrictions and phosphenes using transcorneal electrical stimulation in patients with retinal degeneration. Graefes Arch Clin Exp Ophthalmol, 2006;244:1283-1292
8. Fujikado T, Morimoto T, Matsushita K, Shimojo H, Okawa Y, Tano Y. Effect of Transcorneal Electrical Stimulation in Patients with Nonarteritic Ischemic Optic Neuropathy and Traumatic Optic Neuropathy Jpn J Ophthalmol. 2006;50: 266-273.
9. J. Ohta, T. Tokuda, K. Kagawa, T. Furumiya, A. Uehara, Y. Terasawa, M. Ozawa, T. Fujikado, Y. Tano, "Silicon LSI-Based Smart Stimulators for Retinal Prosthesis," IEEE Eng. Medicine & Biology Magazine 25 (5), 47-59, 2006.
10. J. Ohta, T. Tokuda, K. Kagawa, S. Sugitani, M. Taniyama, A. Uehara, Y. Terasawa, K. Nakauchi, T. Fujikado, Y. Tano, "Laboratory Investigation of Microelectronics-Based Stimulators for Large-Scale Suprachoroidal Transretinal Stimulation (STS)," J. Neural Eng., in press.

11. Terasawa Y, Tashiro H, Uehara A, Saitoh T, Ozawa M, Tokuda T, Ohta J. "The development of a multichannel electrode array for retinal prostheses" J. of Art. Org., vol.9, No.4, pp.263-266, 2006.
12. Fujikado T, Sawai H, Tano Y, Artificial Vision: Vision of a Newcomer. In Artificial Sight, M. S. Humayun, J. D. Weiland, G. Chader and E. Greenbaum (Editors), Springer-New York, in press.
13. 田野保雄 視覚再生、日本の眼科 2006 ; 77 ; 641-646

Electrophysiological Studies of the Feasibility of Suprachoroidal-Transretinal Stimulation for Artificial Vision in Normal and RCS Rats

Hiroyuki Kanda,^{1,2,3} Takeshi Morimoto,^{1,2,4} Takashi Fujikado,^{2,4} Yasuo Tano,⁴ Yutaka Fukuda,¹ and Hajime Sawai¹

PURPOSE. Assessment of a novel method of retinal stimulation, known as suprachoroidal-transretinal stimulation (STS), which was designed to minimize insult to the retina by implantation of stimulating electrodes for artificial vision.

METHODS. In 17 normal hooded rats and 12 Royal College of Surgeons (RCS) rats, a small area of the retina was focally stimulated with electric currents through an anode placed on the fenestrated sclera and a cathode inserted into the vitreous chamber. Evoked potentials (EPs) in response to STS were recorded from the surface of the superior colliculus (SC) with a silver-ball electrode, and their physiological properties and localization were studied.

RESULTS. In both normal and RCS rats, STS elicited triphasic EPs that were vastly diminished by changing polarity of stimulating electrodes and abolished by transecting the optic nerve. The threshold intensity (C) of the EP response to STS was approximately 7.2 ± 2.8 nC in normal and 12.9 ± 7.7 nC in RCS rats. The responses to minimal STS were localized in an area on the SC surface measuring 0.12 ± 0.07 mm² in normal rats and 0.24 ± 0.12 mm² in RCS rats. The responsive area corresponded retinotopically to the retinal region immediately beneath the anodic stimulating electrode.

CONCLUSIONS. STS is less invasive in the retina than stimulation through epiretinal or subretinal implants. STS can generate focal excitation in retinal ganglion cells in normal animals and in those with degenerated photoreceptors, which suggests that this method of retinal stimulation is suitable for artificial vision. (*Invest Ophthalmol Vis Sci.* 2004;45:560–566) DOI:10.1167/iovs.02-1268

Since it was first proposed by Tassicker in 1956,¹ a retinal prosthesis for artificial vision has remained conceptual. During the past decade, however, a retinal prosthesis has become much more realistic and has been supported by recent developments of implantable materials and microelectronics (see reviews^{2–5}). Previous *in vivo* experiments have indicated that impaired parts of the retinal network can be bypassed by electrical stimulation to the retina by microelectrode arrays

implanted in the eye.^{6–10} Results obtained in animal experiments suggest that retinal implantation of stimulating devices hold great promise for restoration of the vision of people with outer retinal degeneration, such as retinitis pigmentosa (RP) and age-related macular degeneration (AMD). Although there have been a few optimistic reports of retinal implants for human patients,^{11–15} there is room for improvement of electrode arrays for clinical application.

Two ways of stimulating the retina for artificial vision are currently well developed. One is subretinal stimulation (SRS), in which a sheet containing a microphotodiode array is inserted into the subretinal space to compensate for lost photoreceptor function and stimulate the outer retinal network.^{6,7,14} The other is epiretinal stimulation (ERS), in which retinal ganglion cells (RGCs) and their axons are stimulated with a multielectrode array attached to the vitreous side of the retina.^{8–13} Either type of retinal stimulation has its own advantages and disadvantages.³ For example, fixing the electrode array is easier with SRS than ERS. In contrast, SRS requires intact optics, whereas ERS does not, and SRS needs a great deal more electrical power than does ERS. Whereas SRS can use retinal circuitry, ERS requires the processing of visual information into specific patterns for the stimulation of RGCs. One common drawback of both types of implants is that implanted electrodes are directly attached to the retina, so that the risk of retinal damage at implantation is inevitable. Although some reports claim that there is no detectable damage to the retina after long-term implantation of microelectrode arrays,^{14–16} surgical difficulties remain if removal or replacement is necessary, both of which are possible. From a clinical viewpoint, it is therefore preferable to have the stimulating electrodes of implants placed away from the retina.

To meet this clinical need, we designed a novel type of transretinal stimulation, with electrodes unattached to the retina. We named it “suprachoroidal-transretinal stimulation” (STS), in which the anodic stimulating electrode is positioned on the choroidal membrane and the cathode is placed in the vitreous body. Because it has been demonstrated that various types of transretinal stimulation can induce field responses in central visual areas,^{17,18,19,20} STS can be expected to activate the retinal network. Our major concern regarding STS is that, because the suprachoroidally placed electrodes are not in contact with the retina, the following disadvantages for artificial vision may result. First, STS may be much less effective than ERS and SRS, resulting in a high threshold for stimulation of the retinal circuitry. The strong electrical stimulation of STS may damage the retina and increase the power load on implanted electronic devices. Second, STS may stimulate a much broader area of the retina than SRS and ERS do, resulting in such a low resolution that artificial vision is impossible.

To test the feasibility of STS for artificial vision, we addressed a critical question in the study reported herein—namely, whether local application of STS can evoke definite responses in the primary visual center that receives direct input from the retina. If this is the case, the localization and threshold of the evoked response are also important issues to

From the Departments of ¹Physiology and Biosignaling, ²Visual Science, and ⁴Ophthalmology, Graduate School of Medicine, Osaka University, Suita, Japan; and ³Nidek Co., Ltd., Gamagouri, Japan.

Supported by Health Sciences Research Grants from the Ministry of Health, Labor and Welfare, and the New Energy and Industrial Technology Development Organization (NEDO), Japan.

Submitted for publication December 11, 2002; revised July 19 and September 22, 2003; accepted October 29, 2003.

Disclosure: H. Kanda, None; T. Morimoto, None; T. Fujikado, None; Y. Tano, None; Y. Fukuda, None; H. Sawai, None

The publication costs of this article were defrayed in part by page charge payment. This article must therefore be marked “advertisement” in accordance with 18 U.S.C. §1734 solely to indicate this fact.

Corresponding author: Hajime Sawai, Department of Physiology and Biosignaling, Graduate School of Medicine, Osaka University, 2-2 Yamadaoka, Suita, Osaka 565-0871, Japan; h_sawai@phys2.med.osaka-u.ac.jp.

examine. To answer this question, we performed acute electrophysiological experiments using the rat retinocollicular system. The superior colliculus (SC) in rats is easily accessible for recording responses to retinal stimulation. Because of the precise retinotopic organization of the SC,²¹ localization of the collicular response could tell us the extent of the retinal area stimulated by STS. From a clinical perspective for further development of STS for human RP, we used Royal College of Surgeons (RCS) rats and normal hooded rats. RCS rats, with inherited retinal degeneration that seems to resemble human RP,²² are well established as one of the best animal models for retinal degeneration.²³ With this retinal dystrophic rat we were able to investigate whether STS can stimulate the residual circuitry of the inner retina and can be used for artificial vision in human RP.

METHODS

Animals

As experimental animals, male hooded rats (Long-Evans; SLC Japan Inc., Hamamatsu, Japan; $n = 17$) from 8 to 14 weeks old and RCS rats (inbred at the Department of Ophthalmology, Osaka University; $n = 12$) from 25 to 30 weeks old were used. All animals were housed under a 12-hour light-dark cycle. All procedures conformed to the ARVO Statement for the Use of Animals in Ophthalmic and Vision Research. Every effort was made to minimize animal discomfort and to use only the number of animals necessary to produce reliable scientific data.

Surgical Preparation

The animals were anesthetized initially with urethane (1.75 g/kg, intraperitoneally). The same anesthetic was administered (0.5 g/kg, intraperitoneally) every 3 hours to keep them anesthetized during the surgical preparations and electrophysiological experiments. A heating pad was used to maintain body temperature at approximately 37°C. Heart rate and electrocardiogram (ECG) were monitored throughout the experiments. The pupils were dilated with a mydriatic (Midorin P; Santen Pharmaceutical Co., Ltd., Osaka, Japan), and the corneas were covered with contact lenses.

After tracheal cannulation, the heads of the animals were fixed stereotaxically. Cerebrospinal fluid was drained through a small incision made into the dura on the obex. Craniotomy was performed on the right side of the temporal bone, and the underlying occipital cortex was removed by gentle aspiration to expose the dorsal surface of the SC. The surface of the SC was filled with mineral oil during the experiments to prevent drying and leakage of current from the recording electrodes. For stimulation of the retina or the optic nerve (ON), the sclera and the ON of the left eye were exposed intraorbitally. After incision of the surrounding tissue and the dura mater, the ON was exposed very carefully to avoid retinal ischemia.

Photoc and Electrical Stimulation

The light source, a photic and sonic stimulator (Nihon Kohden, Tokyo, Japan), was positioned 5 cm in front of the left eye. Stimuli consisting of single flashes were given at intervals of 3 to 5 seconds, and electroretinogram (ERG) or collicular EP was recorded.

For electrical stimulation, a silver-ball-stimulating electrode (suprachoroidal electrode or S-electrode, diameter: 0.2–0.3 mm) was inserted into a small lamellar scleral resection (diameter: approximately 0.5 mm) made at a distance of 1.5 to 2.5 mm from the ON in the upper temporal part of the sclera. The stimulating electrode, electrically isolated from the surrounding tissue with mineral oil, was used as an anode. A cathodic electrode of epoxy-coated stainless wire (vitreous body electrode or V-electrode, diameter: 0.2 mm) with approximately 2 mm of the tip exposed was inserted approximately 4 mm into the vitreous. A single monophasic pulse of electrical current was applied between these two electrodes through an isolator (SS-202J; Nihon Kohden, Tokyo, Japan) connected to an electrical stimulator (SEN-

7203; Nihon Kohden) for 0.05, 0.2, or 0.5 ms, depending on the level of the EP threshold. The range of current amplitude was 5 to 300 μ A. Inward stimulation between the anodic S-electrode and the cathodic V-electrode was used as the standard, and outward stimulation was tested when necessary. The ON was also stimulated with a pair of silver-ball electrodes placed in the intraorbital section, approximately 3 mm behind the globe.

Electrophysiological Recordings

A silver-ball recording electrode (Ag/AgCl, 0.2–0.3 mm in diameter) was moved systematically by means of a hydraulic three-dimensional micromanipulator (MMW; Narishige Science Institute Laboratory, Tokyo, Japan) and placed on the exposed SC surface. A stainless-steel screw was implanted into the occipital bone approximately 1 mm behind the lambda and used as a reference electrode. Responses from the SC were amplified 10,000 times with a band-pass of 15 Hz to 3 kHz. Approximately 50 evoked responses were averaged with a signal processor (LEG-1000; Nihon Kohden).

A flash ERG was also recorded from the left eye using a contact lens electrode (Kyoto Contact Lens, Kyoto, Japan) after a 20-minute scotopic adaptation. ERG responses were amplified 10,000 times with a band-pass of 1 Hz to 3 kHz.

Histologic Analysis

After electrophysiological recordings were obtained from the right SC, a small incision was made with a fine needle at the site where the largest EPs were recorded, as a reference point for reconstruction of the recording sites on the SC. A suture was made at the dorsal pole of the stimulated eye as a marker for retinal orientation. The animals were then deeply anesthetized with a lethal dose of pentobarbitone sodium and perfused intracardially with 0.1 M phosphate-buffered saline (PBS) followed by a fixative (4% paraformaldehyde in PBS). The fixed eye and midbrain were resected for histologic examination under a binocular microscope.

The distance was measured between the optic disc and the position of the S-electrode, which was easily identified by the resection scar on the sclera, and no adjustment was made for shrinkage after fixation. Micrographs of the posterior view of the eye with the optic nerve head, the scar, and the suture at the dorsal pole were taken with a digital camera attached to the microscope. Micrographs were also taken of the dorsal view of the midbrain for reconstruction of the recording sites. Because of shrinkage of the midbrain after fixation, the digital images were sufficiently enlarged that reference incisions for recording sites could be adjusted with their stereotaxic coordinates. The outlines of the SC and the recording sites were then extracted from these adjusted images.

After identification of the position of the stimulating electrode, the eyes were hemisected to make eye cups, which were postfixed and then cryoprotected with 25% sucrose in PBS. Vertical cryosections of the retinal cups were made by means of a freezing microtome (CM1900; Leica, Solms, Germany). These sections were then mounted on gelatinized glass slides and stained with hematoxylin and eosin. Finally, the stained specimens were dehydrated, cleared, and cover-slipped for microscopic analysis of the cytoarchitecture of the retinas.

RESULTS

Field Responses to STS in Normal Hooded Rats

We examined first whether focal STS evokes collicular responses. With a brief pulse of a constant current (0.5 ms, 100 μ A) applied transretinally, evoked potentials (EPs) were consistently obtained from the contralateral SC. Because the amplitudes of the responses depended on the recording site within the SC and the intensity of the current, we first identified the center of the responsive area (CRA) where the largest EPs were recorded for a given intensity of STS. Next, the

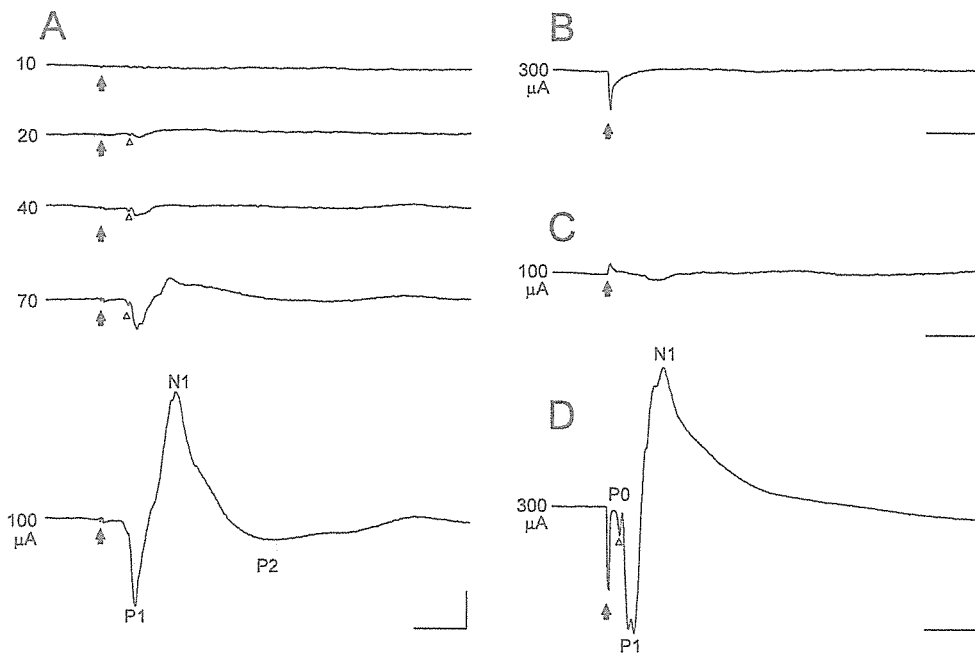


FIGURE 1. EPs recorded from the SC to inward STS (A, B), outward STS (C) and ON stimulation (D) in a hooded rat. Stimulus intensity (in microamps) is indicated at the left of each trace. (A) The EPs consisted of a fast positive wave and a slow negative potential (N1) with a P0 (Δ) that was identified in the second to the fourth trace. The threshold currents for the activation of P1 were 10 to 20 μ A. (B) The EPs to STS disappeared after the ON was severed. (C) In outward STS, the amplitude of EPs decreased. (D) The EPs to the ON also consisted of P0, P1, and P2. Arrows: onset of stimulus. Calibration: (A, B, C) 50 μ V, 10 ms; (D) 100 μ V, 10 ms.

stimulus intensity dependence of the EPs at CRA was examined.

Figure 1A shows a typical series of EPs at the CRA for various intensities of stimulation in a normal hooded rat. With suprathreshold level of STS, the EPs were composed of a sharp positive deflection (P1) followed by a large negative wave (N1) and a small, long-lasting positive wave (P2). The N1 wave was occasionally accompanied by another small negative deflection

(N2; see Figs. 2E, 2F). The ranges of the peak latencies of the P1, N1, and P2 components were 6.7 ± 1.1 ms (mean \pm SD; $n = 14$), 15.3 ± 4.3 ms ($n = 14$), and 34.6 ± 6.5 ms ($n = 10$), respectively. The amplitude of these three components was reduced by tetanus stimulation (at a frequency of approximately 50 Hz), indicating that these responses were postsynaptic (data not shown). At a medium intensity of stimulation (20–80 μ A, 0.5 ms: 10–40 nC), a small positive wave (P0) was

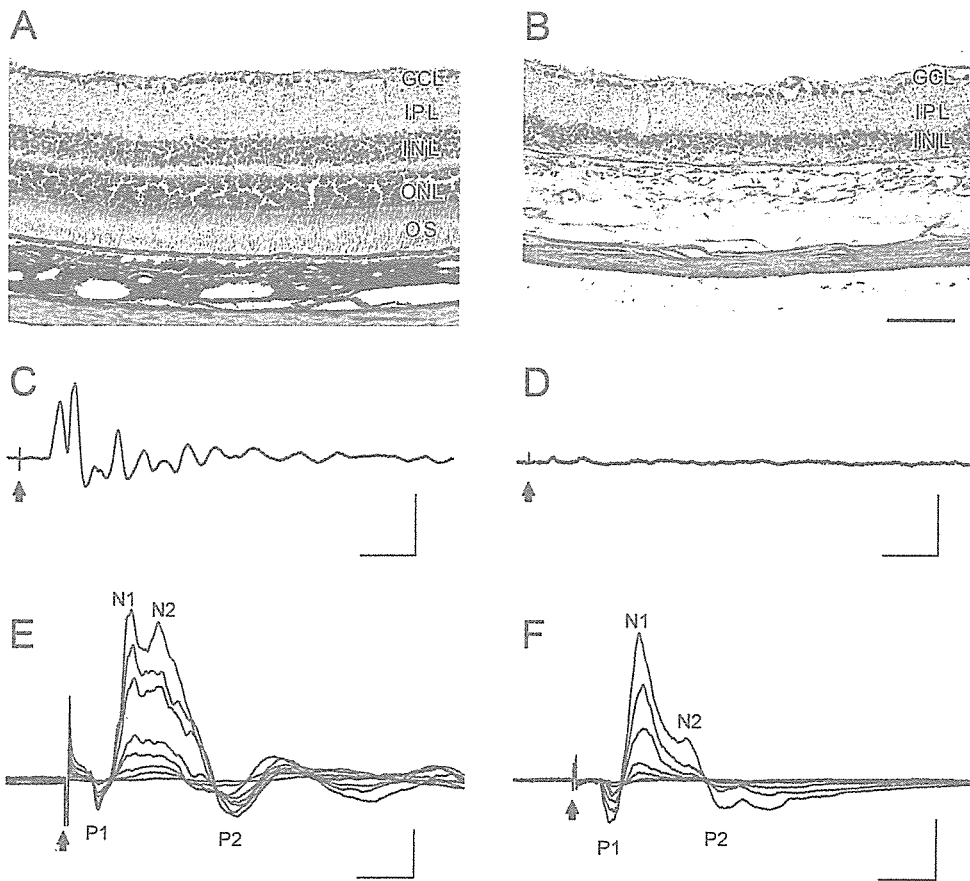


FIGURE 2. Comparison of retinal cytoarchitecture and collicular EPs of hooded and RCS rats. Photomicrographs of hematoxylin-eosin-stained retinal sections of hooded (A) and RCS rats (B) show complete loss of the outer retinal layers in the RCS rat. Flashing-light stimuli generated EPs from the SC of hooded (C) but not RCS (D) rats. The inward STS generated EPs from both hooded (E) and RCS (F) rats. OS, outer segment; ONL, outer nuclear layer; INL, inner nuclear layer; IPL, inner plexiform layer; GCL, ganglion cell layer. Stimulus intensities were 10, 30, 50, 80, 100, 150, 200, and 300 μ A in (E) and 30, 50, 80, 100, 150, 200, and 300 μ A in (F). Arrows: onset of stimulus. Calibration: (C, D) 100 μ V, 50 ms; (E, F) 100 μ V, 10 ms. Scale bar: (A, B) 100 μ m.

often recorded before the P1 wave at a peak latency of 4 to 5 ms, with a peak amplitude of 2 to 10 μV (Fig. 1A; small open triangle). At higher intensities of stimulation, P0 was engulfed by P1 and remained as a notch in the rising phase of the P1 wave. The amplitude did not change with high-frequency stimulations (up to 100 Hz), indicating that the wave reflects the responses of the retinal axon terminals.²⁴ At lower stimulus intensities, the EPs became smaller, and only P0 and P1 remained at 20 μA (10 nC), whereas no response was observed below 10 μA (5 nC). The mean ($\pm\text{SD}$) threshold of STS for evoking EPs was 7.2 ± 2.8 nC ($n = 6$). The EPs were completely abolished after transection of the ON just behind the eyeball (Fig. 1B). Thus, it is unlikely that retinal stimulation directly stimulated the ON and/or the SC.

The threshold of the EPs also depended on the polarity of stimulation. When the stimulating current passed from the V-electrode to the S-electrode (outward stimulation through the retinas), the threshold of the EP dramatically increased from 10 to 60 μA , and, even at 100 μA , only a small P1 was observed (Fig. 1C). In all six cases we examined, switching to outward STS reduced the P1 to N1 amplitude to an average of one tenth. Moreover, this change in stimulus polarity slightly prolonged the peak latency of EPs in two thirds of the examinations. Figure 1C shows the extension of the P1 latency from 7.0 to 9.5 ms.

Field Responses to ON Stimulation in Normal Hooded Rats

To determine whether STS directly activates the ON, we electrically stimulated the ON to record EPs from the CRA of the SC, and compared these EPs with those in response to the retinal stimulation. The EPs for the supramaximal ON stimulation consisted of two positive deflections (P0, P1) followed by a negative deflection (N1), as shown in Figure 1D. The first positive deflection (P0) and the other two components (P1, N1) were identified as presynaptic (ON fiber terminals-derived) and postsynaptic, respectively, because P1 and N1 were completely eliminated by tetanic stimulation, but P0 was unaffected.²⁴ These three components corresponded well to T1, C1, and C2, as designated by Sefton in 1969.²⁵ The mean peak latencies of these components (P0, P1, and N1) were 2.5 ± 0.1 , 4.3 ± 0.4 , and 9.5 ± 0.5 ms, respectively, thus consistently shorter than those of the EPs elicited by the retinal stimulation (P1: $P = 0.029$, N1: $P = 0.035$, Student's paired t -test). The statistically significant differences in peak latency of EPs between STS and the ON stimulation rule out the possibility that STS stimulated the ON directly.

Field Responses to STS in RCS Rats

RCS rats have been used as one of the most effective animal models for human retinal dystrophy, especially RP.²³ To evaluate the suitability of an STS-based artificial retina for clinical application in patients with RP, we used RCS rats to investigate whether STS can bypass their degenerated outer retina and directly activate the residual retinal circuitry.

Figure 2 shows typical results for RCS rats. Histologic examination of RCS rats confirmed severe loss of the outer part of the retinas. The photoreceptor layer completely disappeared in an RCS rat (Fig. 2B) but not in a normal hooded rat (Fig. 2A). Although the inner nuclear layer of the RCS rat was slightly thinner than that of the normal hooded rat, cytoarchitecture of the inner half of the RCS retina seemed to be normal. Some cells with large somata, suggestive of RGCs, were identified in the ganglion cell layer. Moreover, immunostaining for PKC, known as a reliable marker of rod bipolar cells,²⁶ resulted in marked preservation of the bipolar cells in the inner nuclear layer of the RCS rats (data not shown).

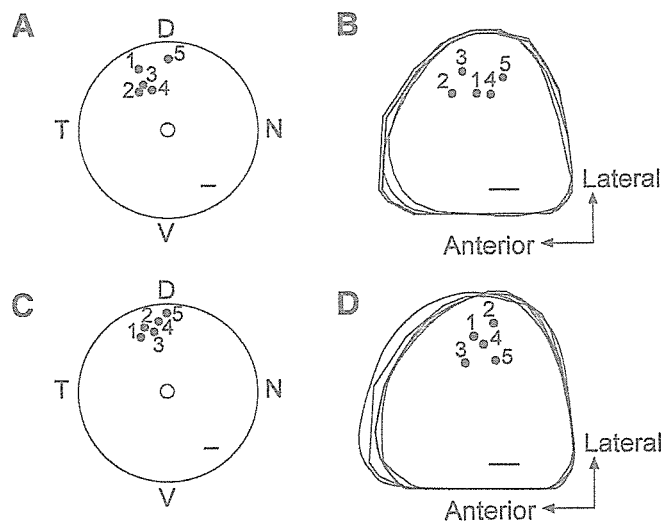


FIGURE 3. Topographic correspondence between the positions of the anodic S-electrodes (A: hooded, C: RCS) and the collicular sites (B: hooded, D: RCS) from which the maximum EPs were recorded in 10 representative animals. Individually numbered filled indicate the retinal positions of the S-electrodes. The corresponding sites with maximum EPs are plotted as filled circles. (A, C) Drawings of the posterior view of the eyes. The circle in the center is the ON. D, dorsal; N, nasal; T, temporal; V, ventral; (B, D) Drawings of the dorsal surface of the SC. Scale bars: (A, C) 1 mm; (B, D) 0.5 mm.

As could be expected from these results, neither ERG (data not shown) nor collicular EP (Fig. 2D) was recorded in response to the flashing-light stimulus in the RCS rat, whereas the same photic stimulus generated conspicuous EPs in the SC of the normal hooded rat (Fig. 2C). The STS (>20 μA for a 0.5-ms pulse) evoked clear field responses on the SC of the RCS rat (Fig. 2F). The EPs consisted of a fast positive wave (P1) followed by a slow negative wave (N1). The peak latencies of the P1 and the N1 were 7.1 ± 1.5 and 13.0 ± 2.8 ms, respectively (mean \pm SD, $n = 11$). When electric current was increased up to 100 μA , the two peaks became very clear. The N1 was occasionally followed by a negative peak (N2) as seen in the case of the high-intensity stimulus. The mean \pm SD of the N2 peak latency in normal hooded rats was 24.6 ± 4.8 ($n = 7$) and 25.6 ± 5.0 ms ($n = 7$) in RCS rats. The EPs to STS in the RCS rats were identical with those in the normal rats (Fig. 2E) in terms of shape and peak latencies of P0, N1 and P1, as well as threshold. The average threshold intensity of the EP in response to STS was approximately 12.9 ± 7.7 nC ($n = 7$) in RCS rats. It was slightly higher than that in normal hooded rats, but the difference was not statistically significant. The effect of changing the polarity of stimulating electrodes was confirmed in RCS rats. The amplitude of EPs decreased up to 8% by outward STS.

Topological Correspondence of Field Responses to the Retinal Stimulation Sites

Because it is well established that retinocollicular projections are topographically ordered,²¹ the collicular positions of the CRA should correspond to the retinal regions in which RGC discharges were elicited by STS. To know whether RGCs below anodic S-electrodes were excited by STS, we examined topological relationship between positions of CRA in the SC and those of S-electrodes. Figure 3 illustrates the results obtained from five normal and five dystrophic rats. In Figures 3A and 3C, individually numbered dots indicate the position of the S-electrode at the dorsotemporal retina at a distance of 1.7 to 2.8 mm from the optic disc. The corresponding CRAs of these animals are plotted as numbered black dots in the outline of

their SCs as based on photographs of the midbrain after fixation (see the Methods section). In Figures 3B and 3D the drawings of these outlines have been placed on top of one other along the midline and posterior edge of the SC. The CRAs were consistently confined to the lateral part of the central SC, which is known to receive inputs exclusively from the upper retina (see Fig. 3 in Siminoff et al.²¹). Thus, there seems to be a topological relationship between the positions of the CRA and the S-electrodes, but not the V-electrodes.

Spatial Extent of Field Responses to the STS

To define the extent of the area that responded electrophysiologically to STS, the EPs were recorded at sites separated by 100 to 200 μm along the rostrocaudal and mediolateral axis of the SC. Because the extent of the responsive area varied with the intensity of STS, it was placed just above the threshold of the EPs at CRA. Figure 4 shows the smallest, intermediate, and largest areas responding to the minimum STS in normal (Fig. 4A) and dystrophic (Fig. 4B) rats. Filled circles indicate recording sites where an EP was obtained and are surrounded by unresponsive sites (horizontal bars). The smallest responsive area was less than a square with sides of 100 μm (Figs. 2, 4A), and the mean \pm SE of the area was $0.12 \pm 0.08 \text{ mm}^2$ ($n = 5$) in the normal rats. In dystrophic rats, the former was less than a square with sides of 200 μm (Figs. 3, 4B), and the latter area was $0.24 \pm 0.12 \text{ mm}^2$ ($n = 5$). Thus, the method of retinal

stimulation used in this study can excite a very small area of the SC, indicating that the retina is focally stimulated.

Resolution of EP to STS at Two Separate Sites

Last, we investigated whether STS of two adjoining areas of the retina can evoke two discrete field responses in the SC of a normal hooded rat. A pair of S-electrodes, S1 and S2, were placed on the eyeball at a distance of approximately 0.7 mm from each other, and these two points were stimulated with an interval of 400 ms. The CRA to STS with the S1 electrode (STS1) was different from that with the S2 electrode (STS2). On the line between these two CRAs, EPs to STS1 and STS2 recorded at intervals of 0.1 mm showed a stimulus intensity of 52 nC (260 μA at a duration of 0.2 ms). Figure 5 illustrates the relative amplitudes of the EPs at each recording site, demonstrating that the response profile to STS1 was spatially differentiated by 0.5 to 0.6 mm from that to STS2. This means that spatial resolution of STS for artificial vision would be 0.7 mm at most.

DISCUSSION

Several studies have demonstrated that ERS or SRS with micro-electrode arrays elicits responses from visual centers.⁶⁻¹⁰ In the present study, we developed a novel means of retinal stimulation for artificial vision (i.e., STS) and demonstrated that focal STS successfully produced localized excitation of the rat SC. This STS was applied through the anode on the fenestrated sclera and the cathode placed in the vitreous body, thus avoiding direct contact of stimulating devices with the retina. Localized EPs were recorded from a small and defined area of the contralateral SC, which corresponds retinotopically to the position of the anode. As with ERS and SRS it can thus be expected that spatially patterned STS through anodes arranged in an orderly manner on the sclera can provide visual centers with essential features of images on the retina.

Suitability of STS for Artificial Vision

By comparison with ERS and SRS, we assessed the suitability of STS for an artificial retina in terms of stimulus efficacy and spatial resolution. High efficacy of stimulation is very important in artificial vision because it results in localizing retinal excitation, preventing retinal damage from electricity, and reducing energy consumption. Efficacy of STS can be assessed by means of the threshold of the stimulation that elicits certain responses in visual centers. The threshold of the collicular response to STS in our study was as low as 5 to 8 nC. Although the threshold of STS is not as low as that of ERS or SRS (for example, 1-36 nC for SRS,⁶ and 14 nC,⁸ 0.1-0.3 nC,⁹ or 0.5-6.0 nC¹⁰ for ERS), it is still low enough for the design of an STS-based artificial retina. In fact, the threshold of STS was quite low when it is taken into account that neither of the stimulating electrodes was in contact with the retina. Probably because electrical resistance of the sclera is much higher than that of the retina and the vitreous, scleral fenestration under the anode may play a role in a highly conductive path, thus contributing to the reduction in the threshold of STS. In fact, we often found during preparation of the animals that the threshold of EPs to STS decreased by up to one half after the fenestration.

Another important question is how a localized area can be stimulated by STS, in that this is crucial for spatial resolution in artificial vision. With minimum stimulus intensity, the area where the EPs were recorded was limited to a few hundred square micrometers, which is roughly 2% of the whole surface area of the SC, or 6.4 mm^2 . With this ratio, the area of the stimulated retina can be calculated as 1.1 mm^2 , assuming that the whole retinal surface area is 57 mm^2 in rats,²⁷ and without

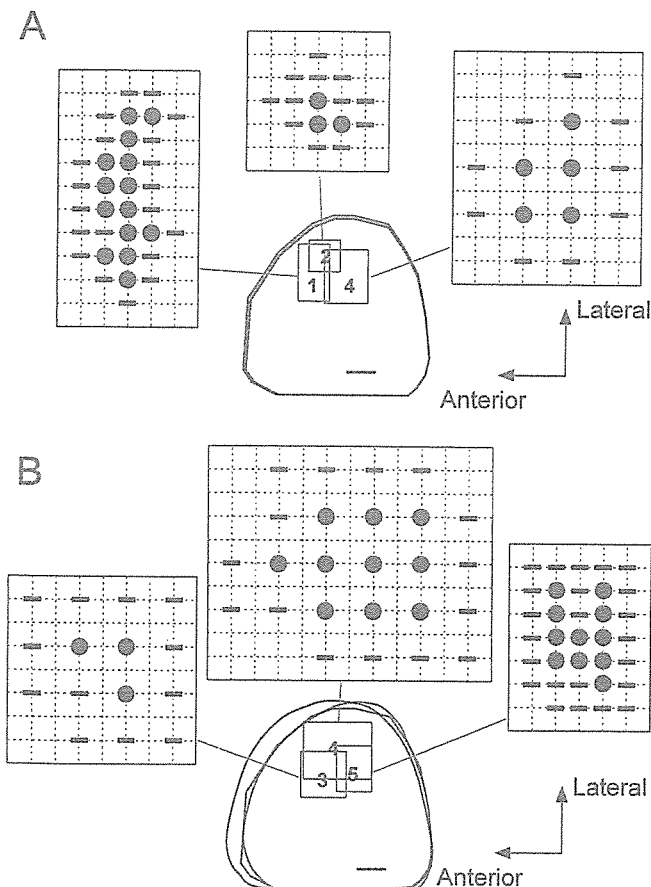


FIGURE 4. Localization of collicular EPs in response to a focal inward STS in hooded (A) and RCS (B) rats. The outlines of the SC surface of three animals were superimposed. The numbers in the squares correspond to those in Figure 3. In each of the expanded squares, the filled circles represent the sites where EPs were recorded, and the horizontal bars show the unresponsive sites. The intensities of STS were just above the threshold: 5 to 8 nC in hooded rats (A) and 10 to 30 nC in RCS rats (B). Scale bar: 0.5 mm; one grid interval, 100 μm .

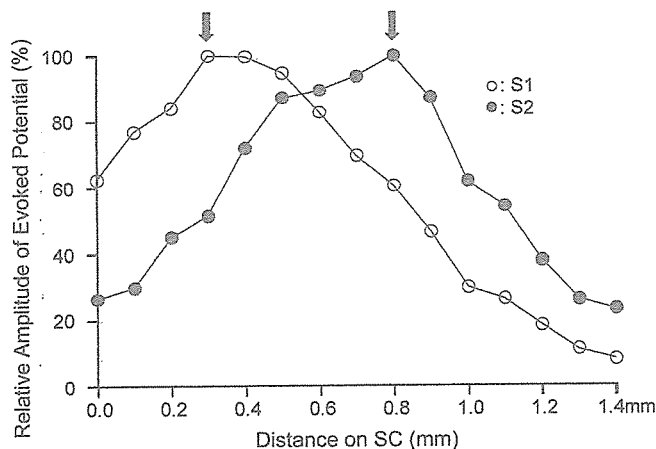


FIGURE 5. Spatial separation of amplitude profiles of EPs in response to inward STS between two different anodic electrodes, S1 (○) and S2 (●). Relative amplitudes of EPs are plotted on the ordinate and positions of the recording electrode on the abscissa. Distance between the two peaks on the surface of SC was 0.5 to 0.6 mm. Arrows: peak response sites to S1 and S2.

taking the retinocollicular magnification factor into consideration. Even such a rough estimation allows us to expect that a single STS to the human eye could activate approximately 1 mm² of the retina.

We also stimulated two retinal sites 700 μ m apart, which resulted in discrimination of two different responsive areas in the SC. The distance of 700 μ m on the human retina corresponds to a visual angle of approximately 2.4°. Therefore, the estimated spatial resolution for STS-based artificial vision seems to be practical, although the resolution in STS is not as good as that for ERS or SRS, which is approximately 1°. Downsizing the anode for STS may improve the spatial resolution.

Compared with ERS and SRS, STS has a major advantage for retinal prosthesis from the surgical point of view. For stimulation, an anodic microelectrode array can be implanted in the fenestrated sclera, and a cathode placed in the vitreous body. Thus, stimulating electrodes will never be in contact with the retina. This configuration of stimulating electrodes would be beneficial in terms of easier and less invasive implantation of the device into the retina. It would also make it easy to remove or replace the implants if necessary. The anodic electrode array would be placed in the intraorbital space, which is relatively large for the implantation of microdevices. This allows for easier design and manufacture of the array with fewer limitations of size and shape than for other implants directly attached to the retina, especially subretinal implants. With STS, moreover, many anodes could be independently implanted instead of a multiple electrode array, so that each of these anodes could be exchangeable individually.

STS in RCS Rats

STS is potentially suitable for retinal prostheses and artificial retinas. This conclusion is ultimately supported by the results obtained in RCS rats, a well-established model of human RP. To the best of our knowledge, this is the first study using RCS rats to demonstrate that localized electrical stimulation to the retina can bypass the degenerated outer retinal circuitry and provide excitation of the visual center, which receives inputs from RGCs.

The EPs to focal STS in the RCS rats were highly similar to those in the normal hooded rats in terms of waveform, peak latencies of the components, and threshold. This similarity suggests that the essential electrophysiological function of the inner retinal circuitry may be maintained even after the degen-

eration of photoreceptors. Histologic analysis proved that the organization of the inner nuclear layer, the inner plexiform layer, and the ganglion cell layer was normal, which agrees with previous findings that indicate that no transneuronal changes occur after the loss of photoreceptor cells.²⁹ On the contrary, there are reports of some abnormalities in horizontal, Müller, and bipolar cells.³⁰⁻³³ Furthermore, it has been found in aged animals that secondary degeneration of RGCs occurs probably due to contraction of intraretinal vessels.³⁴ Feasibility of STS for artificial vision must therefore also be tested in aged RCS rats.

Preservation of normal retinofugal projection after the loss of photoreceptors is one of the prerequisites for an artificial retina. No information is available about the topographic organization of retinofugal projection in case of complete dysfunction of phototransduction, other than an anterograde tracing study that demonstrated that the projection patterns in RCS rats appeared similar to those in their congenic controls, although terminal density was somewhat reduced in dystrophic rats.³⁵ In the present study, EP-recording sites roughly showed topological correspondence to the retinal points stimulated at the anode in the RCS rats as well as in the normal rats. No significant difference was seen between the two strains in the extent of the retinal area activated by STS. These results do not necessarily imply, however, that the topological order of retinofugal projection survives in RCS rats after loss of photoreceptors. Further examination of this point is clearly needed.

Transretinally Stimulated Cells

What types of retinal neurons were stimulated by STS? Photoreceptor cells can be excluded because of our finding that STS evoked collicular responses, not only in normal hooded rats but also in RCS rats with degenerated photoreceptors. Exclusion of photoreceptors as a target of transretinal stimulation was also confirmed by Potts and Inoue,¹⁸ who reported that a change in potential was recorded from the cortex of rats with hereditary photoreceptor degeneration on electrical stimulation applied to the globe. Other lines of evidence about electrically evoked potentials (EEPs) in response to various types of transretinal stimulation also indicate that photoreceptors are not involved in generation of the EEPs.^{19,20,36} Therefore, STS must stimulate the inner retinal cells, such as bipolar cells, amacrine cells, and RGCs, to elicit collicular EPs.

According to electrophysiological principles, the inward transretinal current of STS has a depolarizing effect on the vitreous and a hyperpolarizing effect on the scleral side of every radially oriented retinal cell. Among the inner retinal cells, involvement of bipolar cells and their related synaptic sites in transretinal stimulation was indicated in a few reports using the intact retina.^{20,36} Although the transretinal stimulation in these studies is different from STS, it is likely that STS could also stimulate bipolar cells and their related synaptic sites. The possibility of the RGC as a target for stimulation was excluded by the authors in those studies.^{18,19,36} For example, Stett et al.³⁶ demonstrated in vitro that ganglion cell discharge in response to transretinal stimulation in the chick retina was reduced or eliminated after the application of agents for blocking synaptic transmission. However, when nine neighboring points were stimulated simultaneously (so-called box stimulation), the fast spike and delayed response remained, even after application of a perfusate with a high concentration of Mg²⁺, which suggests that direct stimulation of RGCs may occur when the stimulated area extends within a square with sides of 200 μ m. Because this size is comparable to that of the fenestrated area used in our study, it is possible that STS stimulates RGCs directly. Moreover, using isolated frog retinas, Li et al. have provided evidence of direct excitation of RGCs by transretinal stimulation (Li, et al. *IOVS* 2002;43:ARVO E-Abstract

2844). Further experiments are needed, however, for a fuller understanding of the mechanism of retinal excitation by STS.

Long-Term Efficacy

The present study convinced us that it is feasible to develop an STS-based artificial retina for visually impaired people with degeneration of the outer retina, such as patients with RP and AMD. To reach this goal, however, the long-term stability and biocompatibility of implanted devices for STS have to be thoroughly examined. It is quite possible that regrowth or hypertrophy of the fenestrated sclera would cause deterioration of stimulating efficacy and resolution. Furthermore, prolonged stimulation of the choroid and the retina may induce pathologic changes, such as neovascularization or inflammation of the choriocapillaris. These changes may reduce the effectiveness of STS and even damage the retina. To evaluate the possible chronic effects of STS, we are currently developing surgical procedures for suprachoroidal implantation of a microelectrode array in cats and rabbits.

Acknowledgments

The authors thank Mitsuru Wada for major assistance with many experiments, Jun-Sub Choi for histologic analysis, and Tomomitsu Miyoshi, Tetsuya Yagi, and Masayuki Yamashita for valuable discussion and comments.

References

- Tassicker GE. Retinal Stimulator. U.S. Patent 1956, No. 2, 760, 483.
- Margalit E, Maia M, Weiland JD, et al. Retinal prosthesis for the blind. *Surv Ophthalmol*. 2002;47:335-356.
- Zrenner E. Will retinal implants restore vision? *Science*. 2002;295:1022-1025.
- Rizzo JF, Wyatt J, Humayun M, et al. Retinal prosthesis: an encouraging first decade with major challenges ahead. *Ophthalmology*. 2001;108:13-14.
- Lakhanpal RR, Yanai D, Weiland JD, et al. Advances in the development of visual prostheses. *Curr Opin Ophthalmol*. 2003;14:122-127.
- Chow AY, Chow VY. Subretinal electrical stimulation of the rabbit retina. *Neurosci Lett*. 1997;225:13-16.
- Schwahn HN, Gekeler F, Kohler K, et al. Studies on the feasibility of a subretinal visual prosthesis: data from Yucatan micropig and rabbit. *Graefes Arch Clin Exp Ophthalmol*. 2001;239:961-967.
- Hesse L, Schanze T, Wilms M, Eger M. Implantation of retina stimulation electrodes and recording of electrical stimulation responses in the visual cortex of the cat. *Graefes Arch Clin Exp Ophthalmol*. 2000;238:840-845.
- Walter P, Heimann K. Evoked cortical potentials after electrical stimulation of the inner retina in rabbits. *Graefes Arch Clin Exp Ophthalmol*. 2000;238:315-318.
- Schanze T, Wilms M, Eger M, Hesse L, Eckhorn R. Activation zones in cat visual cortex evoked by electrical retinal stimulation. *Graefes Arch Clin Exp Ophthalmol*. 2002;240:947-954.
- Humayun MS, de Juan E Jr, Dagnelie G, Greenberg RJ, Propst RH, Phillips DH. Visual perception elicited by electrical stimulation of retina in blind humans. *Arch Ophthalmol*. 1996;114:40-46.
- Humayun MS, de Juan E Jr. Artificial vision. *Eye*. 1998;12:605-607.
- Weiland JD, Humayun MS, Dagnelie G, de Juan E Jr, Greenberg RJ, Iliff NT. Understanding the origin of visual percepts elicited by electrical stimulation of the human retina. *Graefes Arch Clin Exp Ophthalmol*. 1999;237:1007-1013.
- Chow AY, Pardue MT, Perlman JI, et al. Subretinal implantation of semiconductor-based photodiodes: durability of novel implant designs. *J Rehabil Res Dev*. 2002;39:313-321.
- Pardue MT, Stubbs EB Jr, Perlman JI, Narfstrom K, Chow AY, Peachey NS. Immunohistochemical studies of the retina following long-term implantation with subretinal microphotodiode arrays. *Exp Eye Res*. 2001;73:333-343.
- Majji AB, Humayun MS, Weiland JD, Suzuki S, D'Anna SA, de Juan E Jr. Long-term histological and electrophysiological results of an inactive epiretinal electrode array implantation in dogs. *Invest Ophthalmol Vis Sci*. 1999;40:2073-2081.
- Lederman RJ, Noell WK. Optic nerve population responses to transretinal electrical stimulation. *Vision Res*. 1969;9:1041-1052.
- Potts AM, Inoue J. The electrically evoked response of the visual system (EER). 3: further contribution to the origin of the EER. *Invest Ophthalmol*. 1970;9:814-819.
- Crapper DR, Noell WK. Retinal excitation and inhibition from direct electrical stimulation. *J Neurophysiol*. 1963;6:924-947.
- Shimazu K, Miyake Y, Watanabe S. Retinal ganglion cell response properties in the transcorneal electrically evoked response of the visual system. *Vision Res*. 1999;39:2251-2260.
- Siminoff R, Schwassmann HO, Kruger L. An electrophysiological study of the visual projection to the superior colliculus of the rat. *J Comp Neurol*. 1966;127:435-444.
- Bourne MC, Campbell DA, Tansley K. Hereditary degeneration of the rat retina. *Br J Ophthalmol*. 1938;22:613-623.
- LaVail MM. Legacy of the RCS rat: impact of a seminal study on retinal cell biology and retinal degenerative diseases. *Prog Brain Res*. 2001;131:617-627.
- Bishop PO, McLeod JG. Nature of potentials associated with synaptic transmission in lateral geniculate of cat. *J Neurophysiol*. 1954;17:387-414.
- Sefton AJ. The electrical activity of the anterior colliculus in the rat. *Vision Res*. 1969;9:207-222.
- Usuda N, Kong Y, Hagiwara M, et al. Differential localization of protein kinase C isozymes in retinal neurons. *J Cell Biol*. 1991;112:1241-1247.
- Hughes A. A schematic eye for the rat. *Vision Res*. 1979;19:569-588.
- Oyster CW. Ocular geometry and topography. In: *The Human Eye: Structure and Function*. Sunderland MA: Sinauer Associates, Inc., 1999:77-109.
- Eisenfeld AJ, LaVail MM, LaVail JH. Assessment of possible transneuronal changes in the retina of rats with inherited retinal dystrophy: cell size, number, synapses, and axonal transport by retinal ganglion cells. *J Comp Neurol*. 1984;223:22-34.
- Chu Y, Humphrey MF, Constable IJ. Horizontal cells of the normal and dystrophic rat retina: a wholemount study using immunolabeling for the 28-kDa calcium-binding protein. *Exp Eye Res*. 1993;57:141-148.
- Hartig W, Grosche J, Distler C, et al. Alterations of Muller (glial) cells in dystrophic retinae of RCS rats. *J Neurocytol*. 1995;24:507-517.
- Hanitzsch R, Zeumer C, Lichtenberger T, et al. Impaired function of bipolar cells in the Royal College of Surgeons rat. *Acta Anat (Basel)*. 1998;162:119-126.
- Peng YW, Senda T, Hao Y, et al. Ectopic synaptogenesis during retinal degeneration in the Royal College of Surgeons rat. *Neuroscience*. 2003;119:813-820.
- Villegas-Perez MP, Lawrence JM, Vidal-Sanz M, et al. Ganglion cell loss in RCS rat retina: a result of compression of axons by contracting intraretinal vessels linked to the pigment epithelium. *J Comp Neurol*. 1998;392:58-77.
- Decker K, Disque-Kaiser U, Schreckenberger M, et al. Demonstration of retinal afferents in the RCS rat, with reference to the retinohypothalamic projection and suprachiasmatic nucleus. *Cell Tissue Res*. 1995;282:473-480.
- Stett A, Barth W, Weiss S, Haemmerle H, Zrenner E. Electrical multisite stimulation of the isolated chicken retina. *Vision Res*. 2000;40:1785-1795.

LABORATORY INVESTIGATION

Transretinal Electrical Stimulation with a Suprachoroidal Multichannel Electrode in Rabbit Eyes

Hirokazu Sakaguchi¹, Takashi Fujikado¹, Xiaoyun Fang¹, Hiroyuki Kanda¹, Makoto Osanai², Kazuaki Nakauchi¹, Yasushi Ikuno¹, Motohiro Kamei¹, Tohru Yagi³, Shigeru Nishimura³, Masahito Ohji¹, Tetsuya Yagi², and Yasuo Tano¹

¹Department of Ophthalmology, Graduate School of Medicine, Osaka University, Suita, Japan;

²Department of Electronic Engineering, Graduate School of Engineering, Osaka University, Suita, Japan; ³Nidek Co., Ltd., Gamagori, Japan

Abstract

Purpose: Several approaches for placing an electrode device for visual prosthesis have been previously proposed. In this study, we investigated if transretinal stimulation from the suprachoroidal space can elicit an electrical evoked potential (EEP) in albino rabbits.

Methods: A flat electrode array (polyimide plate, platinum electrode) was developed and used for this study. After performing a scleral incision at 2–2.5 mm from the limbus and placing an anchoring suture, the array was inserted into the suprachoroidal space in the posterior portion of the eye by direct observation under a microscope. A platinum wire was implanted into the vitreous space as a reference electrode. For electrical stimulation, a biphasic pulse was used. When the electrode was stimulated, the EEP was recorded.

Results: When the electrical stimulation from the suprachoroidal space was applied, the EEP could be recorded with an epidural electrode, and the threshold was $66.0 \pm 32.1 \mu\text{A}$ ($42.0 \mu\text{C}/\text{cm}^2$). Histological examination indicated the absence of major damage to the retina and choroid from the insertion and placement of the array and the electrical stimulation.

Conclusions: Transretinal electrical stimulation from the suprachoroidal space could elicit EEP, suggesting that this approach may be useful for a retinal prosthesis system. *Jpn J Ophthalmol* 2004;48:256–261 © Japanese Ophthalmological Society 2004

Key Words: electrical stimulation, electrode, suprachoroid, transretinal stimulation, visual prosthesis

Introduction

In 1974, Dobbelle et al.¹ demonstrated that a totally blind patient could sense light with stimulation from an electrode in the visual cortex. Since this presentation, the possibility

of artificial vision has been recognized, and many groups have tried to develop a visual prosthesis for blind patients.^{2–18}

Several methods for the placement of an electrode that can stimulate visual neurons were developed. Dobbelle et al. developed the method of stimulating the surface of the visual cortex.^{1,3–5} Several other groups have tried to stimulate the retina with different types of electrodes; some groups have developed subretinal electrodes,^{6–10} and other groups have developed epiretinal electrodes.^{11–18}

There is a rationale for electrically stimulating the retinal neuronal cells with an electrode for visual prosthe-

Received: January 15, 2004 / Accepted: February 2, 2004

Correspondence and reprint requests to: Hirokazu Sakaguchi, Department of Ophthalmology, Graduate School of Medicine, Osaka University, E-7, 2-2 Yamadaoka, Suita 565-0871, Japan
e-mail: sakaguh@ophthal.med.osaka-u.ac.jp

sis. According to Santos et al.,¹⁵ in the retinas of patients suffering from advanced retinitis pigmentosa, 78% of the bipolar cells and 30% of the ganglion cells remain intact.

In this study, we developed a flat electrode array and a method for inserting the array into the suprachoroidal space. We also determined if the transretinal stimulation from this space could elicit an electrical evoked potential (EEP) in albino rabbits.

Materials and Methods

Animals

Five eyes from five Japanese white rabbits, obtained from Hokusetsu (Setsu, Osaka, Japan) and each weighing 2.0 to 2.5 kg, were used in this study. All experiments were performed in accordance with the Association for Research in Vision and Ophthalmology Statement for the Use of Animals in Ophthalmic and Vision Research and the policies in the Guide to the Care and Use of Laboratory Animals issued by the National Institutes of Health, USA.

To anesthetize each rabbit, an intramuscular injection of ketamine hydrochloride (32 mg/kg body weight) and xylazine hydrochloride (4 mg/kg body weight) were used.

Setting of Cortex Electrode

While the animal was under anesthesia, the top of the skull was exposed and drilled at a point on the forehead 8 mm from the suture lambdaeidea and 7 mm right and left of the meridian. Then, screw-type stainless electrodes, coated with silver, were screwed into the skull and attached to the dura mater.¹⁹

Bright-flash Visual Evoked Potential

A bright-flash visual evoked potential (VEP) was elicited before transretinal electrical stimulation to compare its implicit time and waveform with those of the EEP. While the animals were under anesthesia, the eyes were dilated with topical 0.5% phenylephrine hydrochloride and 0.5% tropicamide.

The VEP was evaluated from the screw-type electrode opposite the stimulated eye. VEP was performed with white flashes. The light stimulus was regulated by a stimulator (SLS-3100, Nihon Kohden, Tokyo, Japan), and the flash device (LS-704B, Nihon Kohden) was placed 15 cm above the eye level of the animal to make the basic line of the VEP linear. The VEP waveforms were recorded and calculated by a computer (Neuropack 2, MEB-7202, Nihon Kohden). The energy of the flash was constant at 1.2 J. The results from 50 trials for each eye were averaged and analyzed.

A Flat Electrode Array

A flat electrode array was developed (Fig. 1). The array body was made of polyimide epoxy resin. The length, thickness, and width of the top of the array were 130 mm, 50 μ m, and 2 mm, respectively. Eight round electrodes made of gold were within the array body, not mounted on the body, so that damage to the tissues would be minimal when inserting the array into the suprachoroidal space. The electrodes were connected by copper lines in the array body. The distance between electrodes was 500 μ m.

The impedance of each electrode was examined. The frequency dependency of the impedance is shown in Fig. 2. A 100-mV (peak-to-peak) signal, 500 Hz to 100 kHz AC, was applied to the electrodes during this measurement.

Insertion of the Electrode into Suprachoroidal Space

The pupils were dilated with 0.5% phenylephrine hydrochloride and 0.5% tropicamide. Under a surgical microscope (OPMI 6-S, Zeiss, Oberkochen, Germany), a 2-mm scleral incision was made 2–2.5 mm posterior to the limbus and the choroid was exposed (Fig. 3A). The electrode array was inserted into the entrance of the space between the sclera and choroid through the anchoring suture (Fig. 3B). With a contact lens on the cornea, the electrode array was inserted gradually until the top of the array was in the posterior portion of the eye (Fig. 3C).

Electrical Stimulation and Measurement of EEP at the Visual Cortex

A biphasic pulse was used for the electrical stimulation. The biphasic pulse consisted of one current (suprachoroid to vitreous) and a second opposing current (vitreous to suprachoroid). Both currents had a duration of 0.5 ms. A biphasic pulse with opposite polarization was also used to examine if the direction of the current affected the EEP. The current was varied as follows: 500, 200, 100, 50, 30, 20, and 10 μ A. The current was produced with an electronic stimulator (SEN-7203, Nihon Kohden) and a linear isolator (World Precision Instruments, Sarasota, FL, USA). A platinum wire was implanted into the vitreous space as a reference electrode. With the transretinal stimulation, EEP was investigated with the epidural electrode opposite to the stimulated eye; the EEP waveforms were recorded and calculated by a computer (Neuropack 2). The results from 50 trials for each eye were averaged and analyzed. The threshold and implicit time of the first positive wave were evaluated. The implicit time at a stimulation of 50 μ A was compared with that of the VEP's first positive wave by student's paired *t* test. Statistical significance was assumed when *P* was <0.05; all tests were two-tailed. To make sure the potential originated from the transretinal electrical stimulation within the suprachoroidal space, the same procedures were also performed after removal of the optic nerve underneath the eyeball.

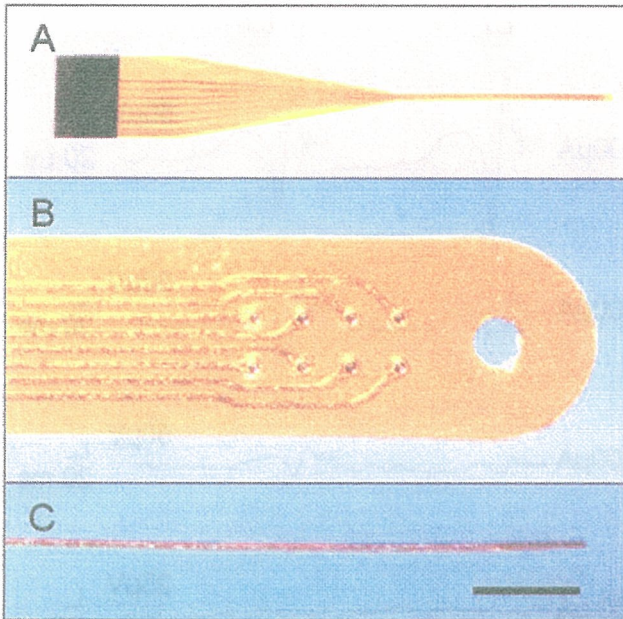


Figure 1A-C. The flat electrode array. **A** The array body is made of polyimide. Its length is 130 mm and the width at its top is 2 mm. **B** High magnification of the top of the array. The electrodes are made of platinum and attached by copper lines in the array body. The diameter of the round electrode is 100 µm, and the distance between electrodes is 500 µm. **C** High magnification of the top of the array. The thickness of the array is 50 µm. The electrodes do not protrude from the array body, and the array is flat. Bar = 1 mm for **B** and **C**.

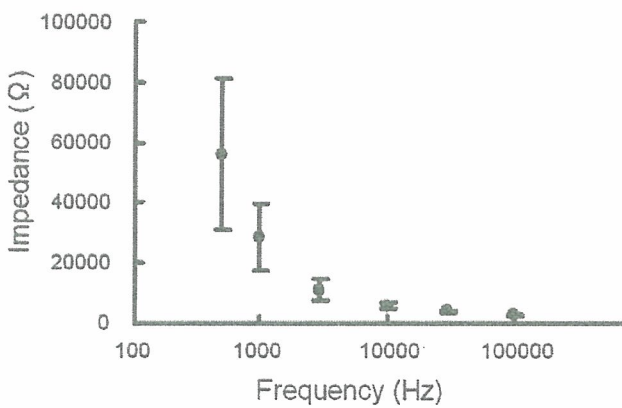


Figure 2. The impedance of the electrodes. Frequency dependency of the impedance is shown. Values are average ± SD, *n* = 3. A 100-mV (peak-to-peak) signal, 500 Hz to 100 kHz AC, was applied to the electrodes during this measurement.

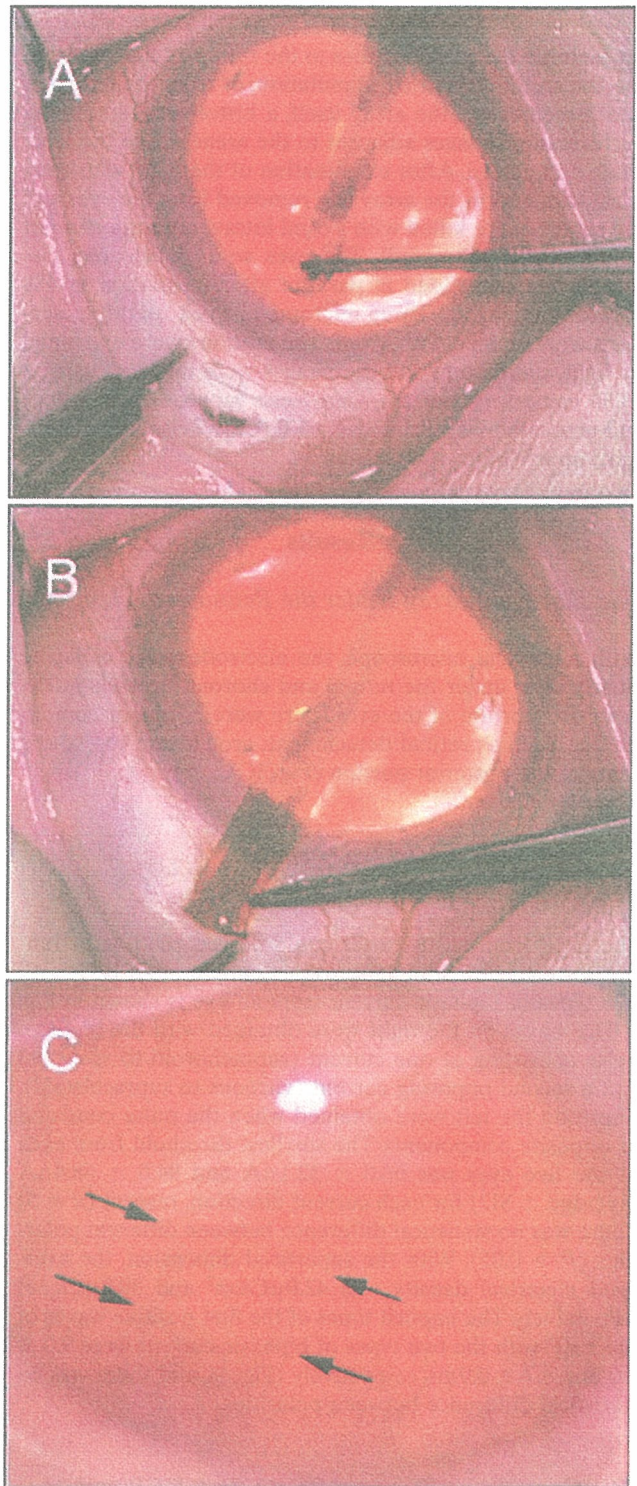


Figure 3A-C. The insertion of a flat electrode into the suprachoroidal space. **A** A scleral incision is made at 2–2.5 mm from the limbus. The choroid is exposed, and the anchoring suture is made. The top of the array is grasped by forceps. **B** The top of the array is inserted into the suprachoroidal space. **C** Under a surgical microscope, the electrode array can be seen clearly under the retina and choroid vessels (*arrows*). Because the array is flat, the damage to the choroidal vessels is minimal, and there are no major complications around the top of the array.